https://doi.org/10.5194/egusphere-2024-3802
Preprint. Discussion started: 7 January 2025

Morphological response to climate-induced flood event variability in a sub-arctic river

Linnea Blåfield[1], Carlos Gonzales-Inca[1], Petteri Alho[1,2], Elina Kasvi[1]

[1]Department of Geography and Geology, University of Turku, Finland

[2]Finnish Geospatial Research Institute FGI, National Land Survey of Finland, Espoo, Finland

Correspondence to: Linnea Blåfield (linnea.m.blafield@utu.fi)

Keywords: Sediment hysteresis, Computational modelling, Flood sequencing, Hydroclimatic

Highlights:

- Flood event type significantly impacts the rivers morphological response
- Increase in multi-peaking flood events affects the river system stability
- Hydrograph shape is associated with specific climatic conditions

Abstract

This study examined the effects of climate-induced flood event variability and peak sequencing on the morphological response of a sub-arctic river. We classified 32 years of discharge hydrographs of a sub-arctic river in terms of their flood event shape variability and peak sequencing, and linked them to seasonal and annual climate conditions. We utilised morphodynamic modelling to examine the effects of the flood characteristics on the morphological response of the river. The findings highlight the critical role that discharge hydrograph shape and sequencing plays in shaping river morphology and sediment transport dynamics. The increasing frequency of double-peaking floods, associated with higher geomorphic activity and sediment loads due to rising temperature and precipitation amount, points to alterations in morphological response of the river channel. This suggests a gradual change in long-term morphological adjustment and potentially a gradual shift in sediment transport regime in the future. These shifts could have long-term implications for river stability, sediment connectivity, and ecosystem dynamics. Even in regions where hydroclimatic changes are not yet fully visible, the flood event characteristics can be evolving and re-shaping the morpodynamics of the river channel. The study underscores the importance of catchment-scale assessments and future research into the combined effects of flood sequencing, sediment transport, and changing hydroclimatic conditions.

https://doi.org/10.5194/egusphere-2024-3802
Preprint. Discussion started: 7 January 2025

1. Introduction

Hydrological variability significantly affects riverine sediment fluxes, especially in cold climate rivers where sediment transport is highly seasonal, occurring predominantly during spring floods (Syvitski, 2002; Favaro & Lamoureux, 2015; Zhang et al., 2022). Snowmelt driven spring floods carry majority of the annual sediment budget and therefore, they define the timing and volume of sediment transport and ultimately the whole river morphology. Currently, cold climate rivers are experiencing rapid shifts of sediment-transport and hydroclimatic regimes (Meriö et al., 2019; Beel et al., 2021; Li et al., 2021; Zhang et al., 2023; Blåfield et al., 2024a). As hydroclimatic conditions evolve, the characteristics of flood events are also changing, with possible implications for sediment transport dynamics. For instance, shift of snow-to-precipitation ratio and changes in the timing and intensity of snowmelt have already altered flood hydrographs i.e. the event shape, magnitude, duration, and sediment transport capacity in cold climate rivers (Wohl et al., 2017; Gohari et al., 2021; Hopwood et al., 2021; Zhang et al., 2022; Blåfield et al., 2024a; Lintunen et al., 2024).

Flood events are usually classified by their generating processes (e.g., intense precipitation, snowmelt, rain-on-snow, ice jamming, dam break etc.), with less emphasis on the event shape and sequences itself. Previous studies (Viglione et al., 2010; Fischer et al., 2019; Gohari et al., 2022) have however reported that the ongoing regime shifts has altered flood event shapes and during the past century multi peaking floods have become more common, not only in central Europe but at high latitude areas as well. In multi-peaking floods, the sequence and duration of different peak types significantly affects sediment transport volume and pattern (Mao, 2018). Therefore, understanding the contribution of flood event sequences to sediment transport is crucial for predicting the climate change impact on fluvial sediment transport and morphological response of the river systems (Mao, 2012; Karimaee Tabarestani & Zarrati, 2015). Especially in cold climate rivers, which have historically had one major snowmelt driven flood and low sediment loads, but with hydroclimatic shift, these regions are becoming hotspots of increased sediment loads (Syvitski et al., 2002; Li et al. 2021; Zhang et al., 2022).

One effective way to evaluate the sediment transport process and morphological response of the river channel is through hysteresis pattern, which describes the sediment transport affected by riverbed structure, sediment composition and availability at different stages of the flow hydrograph (Williams, 1989; Reesink & Bridge, 2011; Gunsolus & Binns, 2017). In cold climate rivers various types of sediment hysteresis have been observed due to highly seasonal and varying sediment availability (Vatne et al., 2008; Kociuba, 2021; Wenng et al., 2021; Zhang et al., 2021; Liébault et al., 2022). Yet, measuring bedload and hysteresis in natural rivers during high flows is still today demanding and easily biased and therefore long timeseries of bedload transport are scarce worldwide (Mao, 2018; Zhang et al., 2023). Thus, we rely on laboratory experiments, computational modelling and field measurements of suspended load when evaluating and measuring the current and predicting the future sediment fluxes and morphodynamic response of the river channels.

The ability to evaluate and predict the effects of climate change on sediment transport rates and morphological response is essential not only for understanding fluvial morphodynamics—such as channel stability and sediment connectivity—but also for a wide range of river engineering and management applications (Mao, 2018; Gupta et al., 2022; Najafi et al., 2021). Therefore, this study

https://doi.org/10.5194/egusphere-2024-3802
Preprint. Discussion started: 7 January 2025

aims to: i) Analyse and classify the variation in flood event hydrographs over the past 32 years in a sub-arctic river, ii) Link the flood events to seasonal and annual climate conditions, and iii) Evaluate the channels morphological response distinctive to each flood event type utilising morphodynamic modelling and sediment hysteresis analysis. We expect to detect linkages between flood event hydrograph shape and climatic conditions as well as individual patterns of morphological response and sediment hysteresis.

2. Study area

Meandering and unregulated Pulmanki River locates in northern Finland and is divided into two separate sections by the Lake Pulmankijärvi. The river is a tributary to Tana River which flows into the Arctic Ocean on Norwegian side of the border. The channel is frozen from October to May, and the seasonal discharge ranges from 0.5 to 100 m^3/s. A spring flood generated by the snowmelt occurs annually in mid-May or early June, lower discharge peaks are associated with precipitation events during July, August and September. The river belongs to subarctic-nival hydrological regime (Lininger and Wohl, 2009) and to Köppen climate class: "Cold, without dry season, but with cold summer" as the area is affected by the great Asian continent and both, Atlantic Ocean and the Gulf Stream.

The area of interest in this study is a 6-kilometre-long reach on the upper course of the Pulmanki River approximately 13 meters above the mean sea level (a.m.s.l). This reach consists of 13 meander bends with a reach sinuosity of 2.4. The river flows through glaciolacustrine and glacio-fluvial sediments deposited on the fjord bottom after the final wasting of Fennoscandian ice sheet (Mansikkaniemi,1967; Hirvas et al., 1988; Johansson et al., 2007). The D50 value of the channel bed material ranges from 0.1 mm to 4 mm and a sandy bedload (D50 0.43 mm) dominates the sediment transport. The channel bed is unvegetated and mobile through the year. The amount of suspended material is minimal (0-180 mg/L), even during the spring flood (Lotsari et al., 2020). The bed morphology is typical for sand bed rivers and consists of dunes, ripples, pools, and riffles.

https://doi.org/10.5194/egusphere-2024-3802
Preprint. Discussion started: 7 January 2025

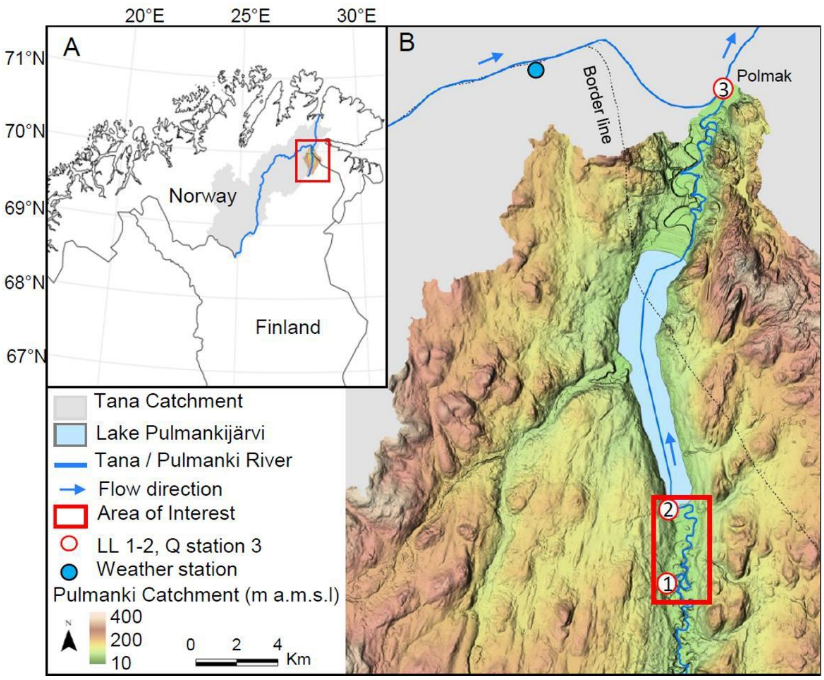

Figure 1. Area of interest. A) The study area's location in the Northern most Finland. B) Model area is marked with rectangle, and the locations of LeveLogger sensors (LL), discharge (Q), and weather station with circular markers. Pulmanki catchment 2x2 m DEM by National Land Survey of Finland.

3. Data & Methods

Discharge hydrographs of the years 1992-2023 were analysed and classified to recognise variability in spring flood event shapes. The most typical flood event of each hydrograph type was selected for morphodynamic modelling to evaluate the channels morphodynamic response and sediment transport dynamics. The flood events extracted from the classified hydrographs were linked with climate data from equivalent time period to examine possible connections between climate and flood event shapes. Mann-Kendall trend test was run on the hydroclimatic variables to detect possible trends in the time-series. Continuous discharge and water level monitoring has been conducted in Pulmanki River since 2008 during open water season (May-September). The Pulmanki River discharge time-series was complemented with Polmak discharge station data from Tana River (Fig. 1) to cover the whole 32-year time period. Sediment and bedload transport samples were collected during the spring and autumn field work from various discharge conditions.

3.1 Hydrograph measurements and generation

Hydrographs of open water season were generated utilising a combination of data sources. For the years 2008-2023, rating curves based on combination of field data were generated; water pressure sensor data (Levelogger 5, Solinst), water level data measured with Virtual Reference Station-Global Navigation Satellite System (VRS-GNSS), and discharge data measured with Acoustic Doppler Current Profiler (ADCP M9, Sontek). Each year, the water pressure sensors were placed into the

https://doi.org/10.5194/egusphere-2024-3802
Preprint. Discussion started: 7 January 2025

upper Pulmanki River after ice-breakup in spring and picked up before winter (see locations in Fig 1). This way the sensors covered the whole open water season and seasonal variations of water pressure, water level and discharge with 15 minute interval. The location of the sensors was identical each year. To compensate atmospheric influence on water pressure, an air pressure sensor data from Solinst Barologger was subtracted from the water pressure readings. During field campaigns in May and September water level and discharge were measured daily from the LeveLogger locations for creating rating curves between LeveLogger pressure, water level (WL) and discharge (Q). Based on the rating curves, a 3rd order polynomial function was selected for calculating annual hydrographs of open water seasons (Figure 2A).

For the years 1992-2007, openly available daily discharge data from Polmak measurement station, maintained by the Norwegian Water Resources and Energy Directorate (NVE) was used (see location in Fig 1). The station is located in the main channel of Tana River at the spot where Pulmanki River discharges into Tana and has been operating since November 1991 until today. The discharge for Pulmanki River was derived from the Polmak station data using rating curve and 3rd order polynomial function between the Polmak station discharge (Q) and Pulmanki River Q of 2008-2023 derived from the LeveLoggers (Figure 2B). The final hydrographs of Pulmanki river are based on these two equations and data sources. The hydrographs were validated against ADCP discharge measurements from Pulmanki River main channel. These measurements were excluded from the rating curve creation. See the details of error metrics in Table 1.

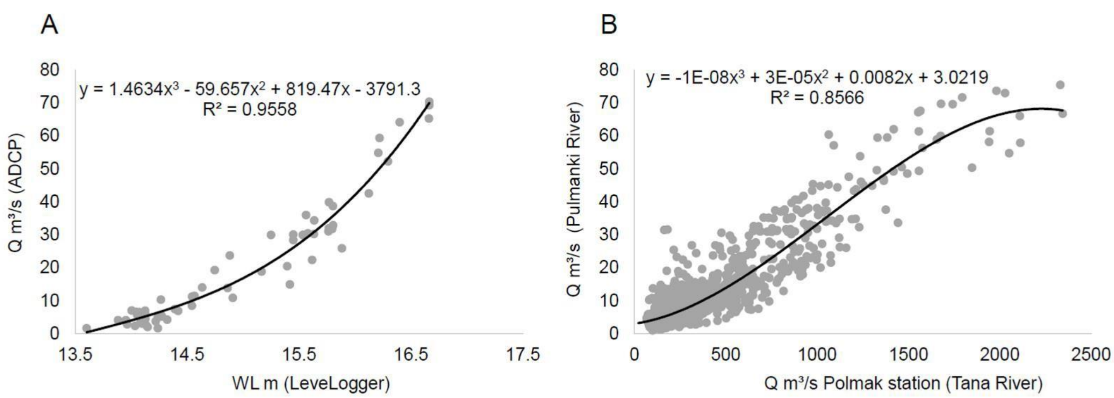

Figure 2. Rating curves for Pulmanki River hydrographs. A) Regression curve of discharge measurements (y) and LeveLogger water level (x) in Pulmanki River 2008-2023. This polynomial function A was used to calculate hydrographs for years 2008-2023 B) Regression curve showing the relationship between the discharge in Pulmanki (y) and Polmak (x) during 2008-2023. This polynomial function B was used for calculating Pulmanki River discharge for years 1992-2007.

https://doi.org/10.5194/egusphere-2024-3802
Preprint. Discussion started: 7 January 2025

Table 1. Error metrics of the final hydrographs derived from two different data sources: LeveLogger discharge data and Polmak Station discharge data.

Pulmanki River Q Derived from:	Min. Error (m^3/s)	Max. Error (m^3/s)	Mean Error (m^3/s)	MAE (m^3/s)	SDE (m^3/s)	r	R2	n
LeveLogger	-9.59	10.73	-0.24	2.92	3.74	0.94	0.89	152
Polmak Station	-51.48	20.34	-0.39	2.59	4.65	0.89	0.80	1804

3.2. Hydrograph classification

The hydrographs were classified into distinct flood event types based on the peak shape in Python. A threshold value of 23.46 m^3/s (75th percentile, p75 discharge) for flooding was set to classify significant spring flood events during May and June. The definition for high and low flood event was set to be either above or below the mean flood discharge of 40 m^3/s, respectively. The event classification was done by estimating different flood peak features such as peak timing, prominence, peak height, and peak event duration. First, Savitzky-Golay smoothing filter was applied to the dataset to reduce noise and enhance the detectability of flood peaks. This was accomplished using the Savgol_filter function from the `scipy.signal` module, with a window size of 11 and a polynomial order 3. Peak shapes within the smoothed data were identified and classified into distinct flood events using the `find_peaks` function from the `scipy.signal` module.

Four different event types were detected: A) High one peak ($Q>40$ m^3/s), B) Low one peak ($Q<40$ m^3/s), C) Two separate peaks (Q>p75, Q<p75, Q>p75) and D) Wavy peak (two Q>p75 peaks) (Figure 3A-D). For modelling purposes, the most typical event of each type was selected (red solid line in Fig. 3A-D). The precipitation driven discharge peaks in July, August and September were left out of the analysis as none of them exceed the flood threshold discharge of p75. In addition, previous studies indicate that the majority of high latitude rivers transport most of their annual load during the main flood event, i.e., spring flood (Syvitski, 2002; Zhang et al., 2022; Blåfield et al., 2024b).

https://doi.org/10.5194/egusphere-2024-3802
Preprint. Discussion started: 7 January 2025

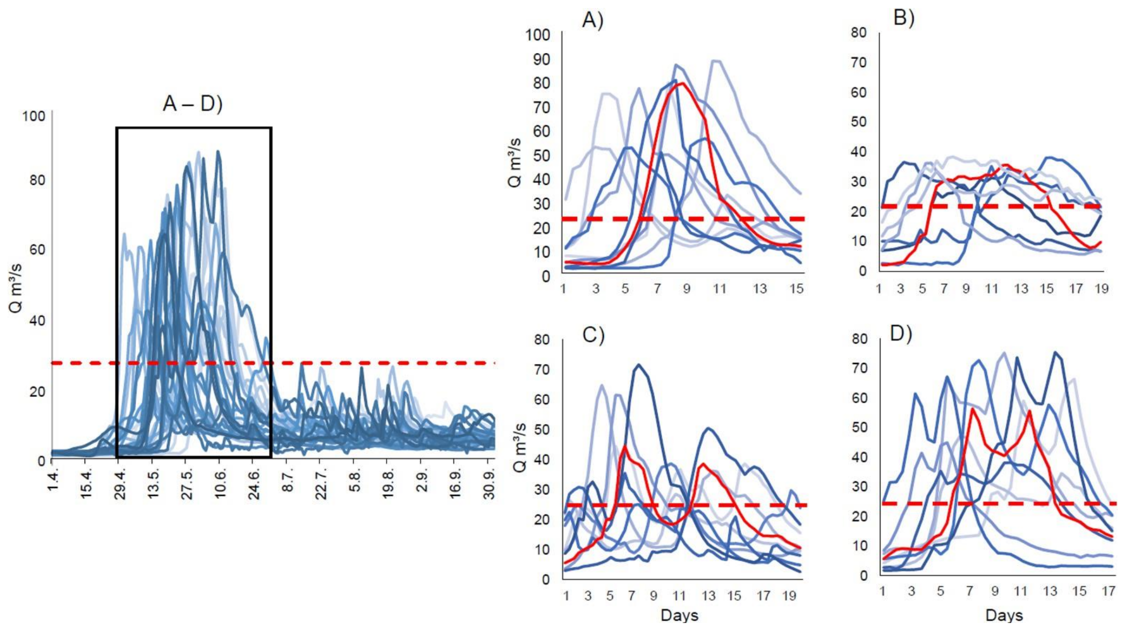

Figure 3. All generated hydrographs in 1992-2023. The classification led to four distinct flood event shapes: A) High one peak flood, B) Low one peak flood, C) Two separate peaks, and D) Wavy peak. The solid red hydrograph is the most typical flood event of each shape which was thus used in the morphodynamic model. Red dashed line is the 75th percentile threshold discharge for flood.

3.3. Hydroclimatic data and trend analysis

Climate data from the Nuorgam weather station (see location in Fig. 1), 11 metres above the mean sea level and 17 kilometres North from the Pulmanki River, was downloaded from the Finnish Meteorological Institutes open data service. Daily Total, Min, Mean and Max temperature, precipitation, and snow depth data of years 1991-2023 was selected for the analysis as these variables are closely related to the hydrological properties of rivers (Veijalainen et al., 2010; Irannezhad et al., 2022). Annual Min, Mean, Max and Total values were derived from the daily data and used in the trend analysis (Fig. 4). In addition, duration of snow cover, precipitation events, and occurrence of Extreme snow/precipitation events (95^{th} percentile) were derived for the trend analysis. For detailed analysis of springtime trends, the corresponding measures were derived for March, April, and May as well. Only one weather station was included in the analysis as other stations are located 50-100 kilometres away with over 100-meter elevation difference to the area of interest. The year 1991 was included in the climate time-series as the analysis was conducted on hydrological years instead of calendar years.

The Mann-Kendall (MK) trend test was carried out on all climate variables with α = 0.05 significance level identifying statistically significant monotonic trends. In addition to climate variables, the MK-trend test was run on the classified flood hydrographs to examine trends in the occurrence interval, timing, volume, and duration of each flood event hydrograph type. Possible serial correlations were removed by using Hamed & Rao (1998) M−K modification, which is explained in detail in e.g., Daneshvar Vousoughi et al., 2013; Jhajharia et al., 2014). The effect of outliers on the trend was neglected by using a non-parametric linear regression Sen's slope estimator (Sen, 1968).

https://doi.org/10.5194/egusphere-2024-3802
Preprint. Discussion started: 7 January 2025

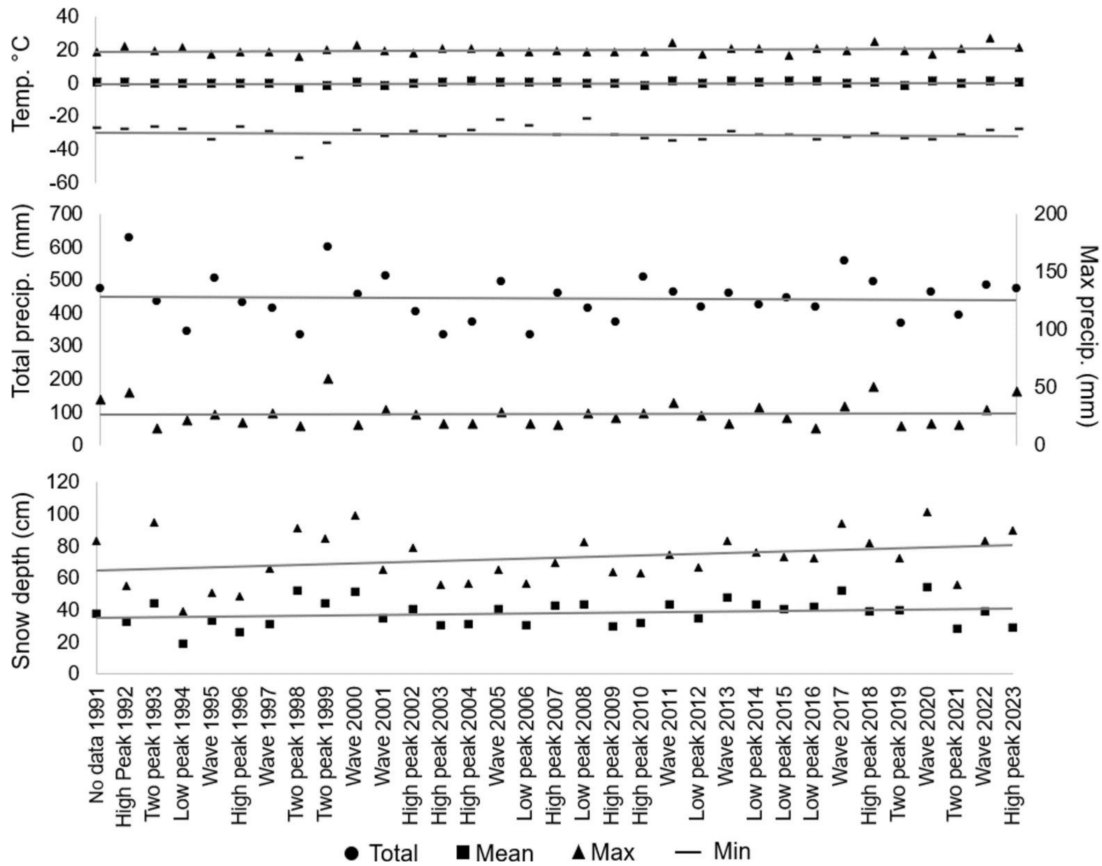

Figure 4. The annual climate time-series of the 32-year time period derived from the daily data. The corresponding flood event types are marked on the x-axis.

3.4. Sediment and bedload sampling

Both grab samples with Van Veen sediment sampler, and bedload samples with Helley-Smith sampler were collected from the riverbed. A total of 70 grab samples (ca. 500 g) and 24 bedload transport samples during various discharges (sampling time 6 minutes) were collected from the area of interest. The samples were dry sieved using half-phi interval and the amount of material in each sieve was weighted. Sample statistics were calculated in GRADISTAT-program (Blott & Pye, 2010) using Method of Moments which is based on logarithmic distribution of sample phi sizes. GRADISTAT utilises its own scale with only four classes (Silt, 0.002–0.063 mm; Sand, 0.063–2 mm; Gravel, 2–64 mm; and Boulders, 64–2048 mm). The results of sediment and bedload sampling were utilised in the morphodynamic model as multiple sediment fractions, spatially varying Manning's Roughness parameter, and for calibrating and validating the sediment transport rates (see details in Blåfield et al., 2024b).

https://doi.org/10.5194/egusphere-2024-3802
Preprint. Discussion started: 7 January 2025

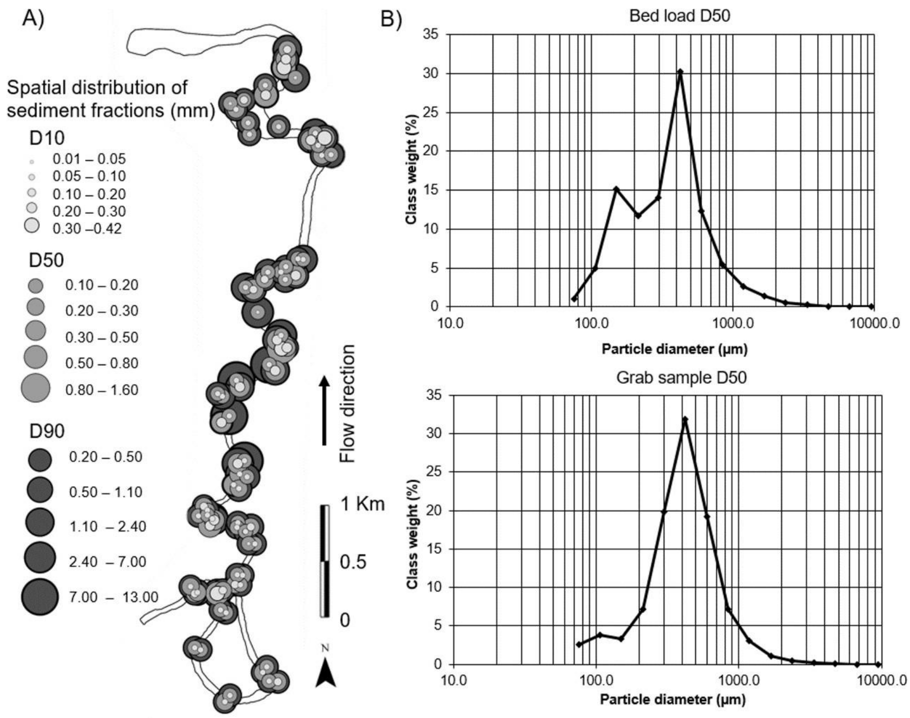

Figure 5. A) Spatial distribution of sediment fractions D10, D50 and D90 based on the collected field samples. B) D50 particle diameter distribution of all the collected bedload and grab samples in micrometres.

3.4 Morphodynamic modelling

The authors have previously presented and validated the model used in this study (Blåfield et al., 2024b). A depth-averaged morphodynamic model with curvilinear, unstructured grid of 2x2 meter cell size was built utilizing FLOW 2D-module of Delft3D software. The models' geometry was based on a digital elevation model derived from Structure-from-Motion, specific details can be found in Blåfield et al., (2024b) and general from Micheletti (2017). Multiple sediment fractions and spatially varying Manning's Roughness was used based on the field samples since it significantly enhances the predicted morphodynamics (Kasvi et al., 2014). The model solved independently the morphology based on the van Rijn (1993) approach, and the transport boundary conditions based on the Neumann law. This way the model adjusted the inflow supply and concentration equal to those inside the model and very little accretion occurred near the boundaries. The default scheme for dry cell erosion of banks was used. The parametrization of the model, calibration and validation details can be found in Blåfield et al., (2024b). In this study, four different flood event hydrographs (A-D in Table 2.) were run over the same starting geometry with identical sediment composition to evaluate transport conditions, hysteresis, and channels morphological response to the flood events shape and sequences. The spin up and output interval were both set to 720 minutes to better match the time frame of this study. The model morphology was updated at each time-step. Later, the geomorphic activity for each flood event type was calculated from the model outputs based on the total mobilised volume of sediment within the inundated area.

https://doi.org/10.5194/egusphere-2024-3802
Preprint. Discussion started: 7 January 2025

Table 2. The details of each model run. The flow conditions of flood events A-D are based on the hydrograph classification in chapter 3.2. The morphological parameters are based on the sediment and bedload sampling on the field.

Event	Duration (days)	Peak Q m^3/s	Total Q Volume m3	Sediment Supply	Morphology	Sediment composition
A	7	80	29 868 586	Feeding	Sand bed	Sand, Gravel
B	13	35	34 851 505	Feeding	Sand bed	Sand, Gravel
C	14	48	26 2383 45	Feeding	Sand bed	Sand, Gravel
D	9	60	31 20 1609	Feeding	Sand bed	Sand, Gravel

4. Results

4.1 Hydroclimatic conditions and flood event type variability

The comparison of flood events A-D and the prevailing climate conditions showed that each flood event type could be linked to slightly different climate conditions (Fig. 6). High one peak flood events (A) had the coldest annual and spring temperature conditions, with relatively high annual and spring snow depth (Fig. 6). High annual and low springtime precipitation were linked with high peak floods. Low one peak flood events (B) exhibited the most stable conditions, with very little variation (Fig. 6). Its spring temperatures were slightly above freezing, and it experienced moderate conditions in snow depth and precipitation amount in both annual and spring time. Flood events with two separate peaks (C) showed the lowest snow sums, moderate mean temperature, and precipitation amount (Fig. 6). In addition, it had more variability than event B but did not reach the extremes seen in events A or D. Finally, the wavy flood events (D) experienced the warmest temperatures, high amount of snow, and high levels of both, annual and spring precipitation (Fig. 6). However, this flood event type experienced a wide range of variation, particularly in spring variables but overall, the conditions were wettest, snowiest, and warmest of all.

https://doi.org/10.5194/egusphere-2024-3802
Preprint. Discussion started: 7 January 2025

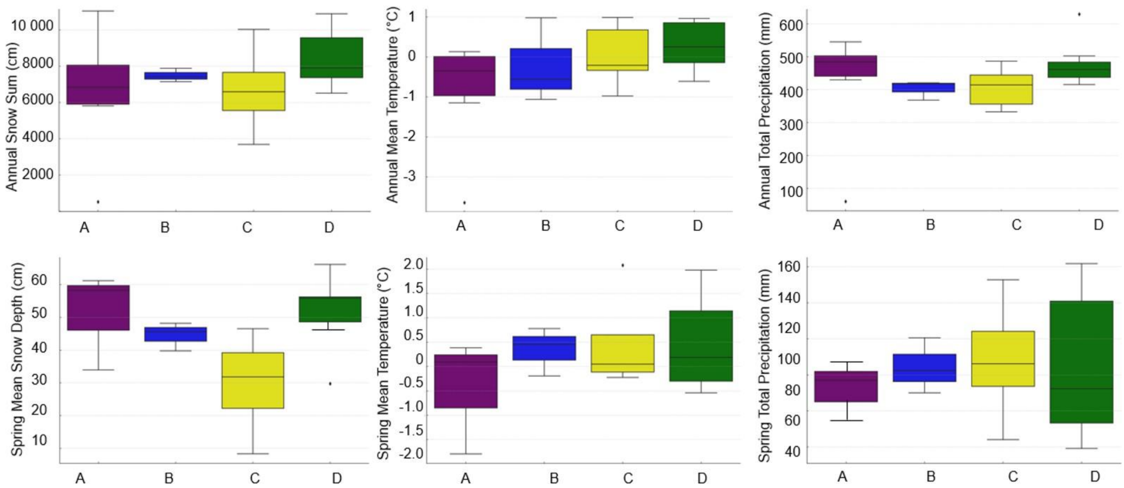

Figure 6. Distribution, median and variation of climate variables associated with each flood event type. Upper row consists of annual data and lower row of spring quartile data (April, May, June). Types A and D were linked to high snow amount. Type B had the lowest variability, whereas Type C had the highest variability. In general, there were more variation in spring variables than annual variables, which implicates that the hydroclimatic conditions preceding the spring flood impact the flood event type more than the prevailing spring conditions.

The wavy (D) and high one peak (A) events appeared the most frequently, both occurring 10 times within the 32-year time-series. The wavy event D had an average duration of 9 days whereas high one peak event A lasted 7 days on average. Low one peak event B occurred 7 times and had the longest average duration of 13 days. Finally, the event C of two separate peaks was the least frequent type with 5 occurrences lasting 14 days on average. No significant trends were observed in recurrence interval, duration, volume, or timing of the flood event types within the time-series (Fig. 7). Trend analysis on the climate variables solely revealed that in snow-related variables (mean, maximum, and extreme snow), all trends were positive with statistically significant increase in both annual (square marker) and spring time (circle marker) trends, particularly for maximum and mean snow depth. Snow days, however, showed non-significant weakly negative trends (Fig. 7). Temperature trends were mostly positive, with significant increases in both annual and spring maximum temperature, indicating warming, especially for the annual maximum temperature (Fig. 7). Minimum temperature showed no significant trend in annual or spring time data. Precipitation-related trends were more variable. Minimum precipitation exhibited mostly negative trends, while mean precipitation showed some significant increases in both annual and spring trends (Fig. 7). Maximum and extreme precipitation trends were annually non-significant but showed slight increases. Spring extreme precipitation however, showed significant decreasing trend. Number of precipitation days had no significant trend. Overall, snow metrics showed increasing trends and both annual and spring time temperatures were increasing, however, precipitation parameters indicated variable trends with least significance.

https://doi.org/10.5194/egusphere-2024-3802
Preprint. Discussion started: 7 January 2025

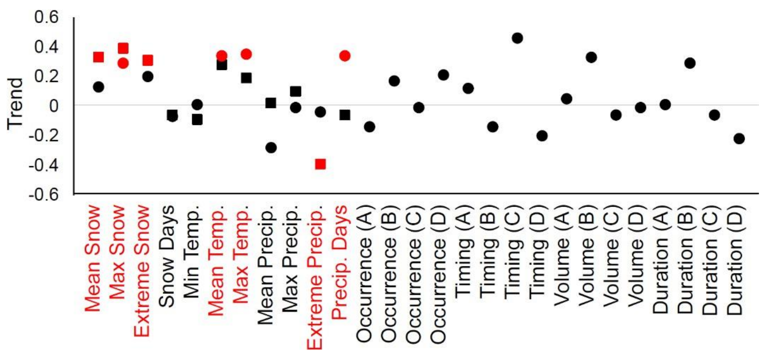

Figure 7. The MK-trend test results of the climate-related variables during the 32-year study period. Red markers indicate statistically significant trends and black markers non-significant. Square markers represented annual trends, while circles represent seasonal trends in spring.

4.2 Morphological response to sediment transport hysteresis

The four different flood event types were modelled with identical starting morphology. The results indicate the event shape significantly impacted the morphological response and sediment transport hysteresis, rather than the total discharge volume of the flood event. The amount of total transported sediment (TTS) and the type of sediment hysteresis differed in each of the event shapes. Wavy event (D) had the largest volume of TTS. The first peak was 59 % and the second peak 41 % of the events TTS. The first peak had therefore 28 % higher transport rate than the second peak. In a flood event of two separate peaks (C), the first peak composed 63 % and the second peak 37 % of the TTS, respectively. The transport rate of the second peak was thus 42 % lower than in the first peak. The TTS of event C was 17 % lower than TTS of event D. High one peak event (A) had 4 % lower TSS volume than event D, and 11 % higher TTS than event C. The low one peak event B had 30 % lower TTS than the High one peak event A, and 20-32 % lower TSS than the double peaking events C and D, respectively.

All the events experienced mainly counterclockwise sediment hysteresis (transport peak occurring after the peak flow) (Fig. 8A-D), meaning the sediment transport lags the changes in discharge and flow conditions. However, the sediment hysteresis loops differed in complexity and shape depending on the flood event type. The single peak events A and B had simple counterclockwise loop-shaped hysteresis, with sediment transport occurring after the peak discharge (Fig. 8A-B). Event C had more complex hysteresis including multiple counterclockwise loops, indicating that the sediment mobilised in the first event was likely settled between the peaks as the second peak had significantly lower TTS (Fig. 8C). In the wavy event D, the first peak hysteresis was counterclockwise, but the second peak sediment occurred before the second peak discharge, leading to clockwise hysteresis (Fig. 8D). This led to a complex hysteresis indicating variability in sediment mobilisation processes and availability. Each of the events experienced higher TTS values during the falling limb than in the rising limb with the corresponding discharge value, indicating that the sediment transport volume was not directly proportional to discharge (Fig. 8A-D). This discrepancy between TTS and discharge during the falling limb highlights the role of delayed and progressive sediment mobilisation and

https://doi.org/10.5194/egusphere-2024-3802
Preprint. Discussion started: 7 January 2025

delayed morphological response of the bed forms. This implies that the event shape has a notable influence on the sediment transport hysteresis and therefore on the riverbed morphology.

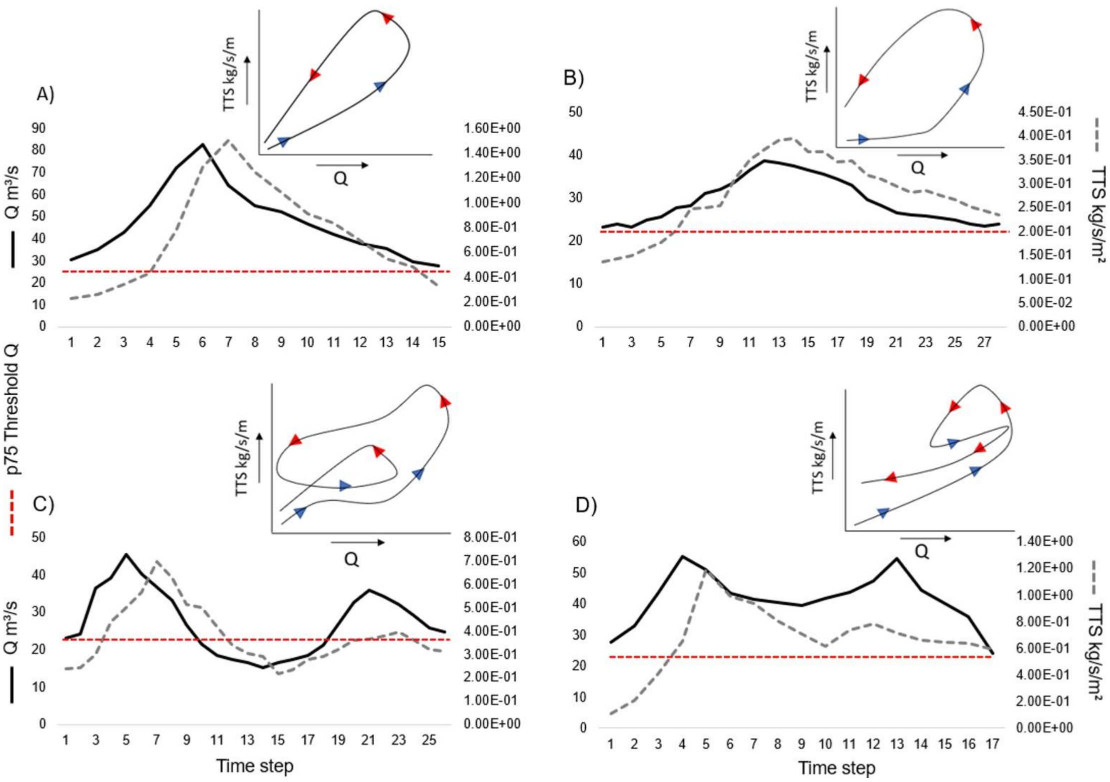

Figure 8. The modelled flood event hydrographs and sediment load at each timestep. On the upper right corner of each graph is the sediment hysteresis of the event type. The blue arrows indicate rising limb and red arrows falling limb of the flood. The red dashed line shows the threshold p90 discharge. A) High one peak event and sharp counterclockwise sediment hysteresis. B) Low one peak event and wide counterclockwise sediment hysteresis. C) Event with two separate peaks and counterclockwise sediment hysteresis with a loop. D) Wavy type event and hysteresis loop with counterclockwise and clockwise directions.

Each event demonstrated distinct patterns of morphological response (Fig. 9A-D), influenced by variations in sediment hysteresis, stream power and flow velocity. Event A had the second highest total volume of mobilised sediment and geomorphic activity (Fig. 9A). The event experienced the most significant erosion throughout the whole reach, whereas deposition areas were localised. The highest rates of stream power were observed in this event, with values exceeding 24 W/m², and a mean flow velocity of 0.61 m/s, which both contributed to the substantial erosion and the overall net sediment loss of -14 772 m³. The sediment feeding from upstream could not compensate to the balance. In contrast, event B experienced the lowest geomorphic activity, with a more balanced distribution of erosion and deposition across the river reaches imitating classic meander behaviour and morphological response with distinct riffles and pools (Fig. 9B). The stream power was significantly lower than in event A, with most values under 10 W/m² with a mean flow velocity of 0.36

https://doi.org/10.5194/egusphere-2024-3802
Preprint. Discussion started: 7 January 2025

m/s. These conditions likely allowed the fed, eroded and transported sediment to settle within the reach, resulting in a net sediment gain of 5 482 m³.

Event C was rather balanced event with even distribution of erosion and deposition and the lowest net change with a gain of 1 132 m³ of sediment (Fig. 9C). The upstream section experienced the heaviest erosion whereas the downstream section gained the most sediment, middle reach experienced minor changes. The stream power for event C was moderate with values mostly under 16 W/m², the value of 20 W/m² was only occasionally exceeded. Event D had the most fragmented morphological response with small-scale areas of both erosion and deposition distributed throughout the river reach (Fig. 9D). The stream power distribution of event D was closer to that of event A, with values reaching over 20 W/m², and a mean flow velocity of 0.54 m/s. Despite this higher energy, event D produced a more balanced sediment budget, though it still resulted in a net sediment loss of -6 267 m³. The geomorphic activity per unit area was highest for events A and D, both of which showed considerable erosion and sediment mobilization but ended up with different morphological response of the riverbed. Events B and C showed lower geomorphic activity, with a tendency toward sediment deposition rather than erosion. The pattern of morphological change caused by the modelled flood events were thus linked to the peak shape and sequences and the following sediment hysteresis pattern, which had significant effect on the morphological response of bed forms. Events A and B experienced distinct areas of erosion and deposition whereas in the double peaking events C and D the changes were more irregular and fragmented around the reach.

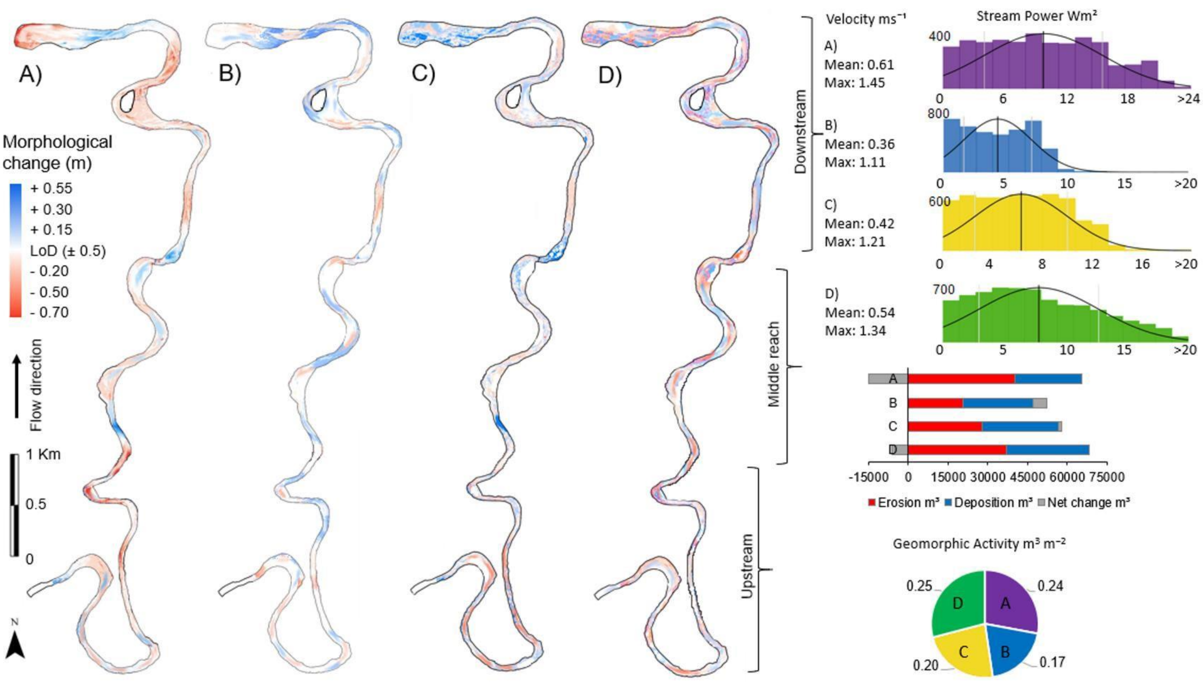

Figure 9. Morphological adjustment of each flood event (A-D) in left panel: A) Distinct areas of heavy erosion and deposition. B) Less prominent morphological changes but distinct areas of erosion and deposition. C) More complex morphological changes patched around the river reach. D) Heavy erosion and deposition spread complexly within the reach. Right panel: A-D events mean and max

velocity, histograms of stream power (x) distribution within number of model cells (y), volume of erosion, deposition, and net change, and geomorphic activity.

5. Discussion

5.1. Flood event types and hydroclimatic conditions

The observed trends in climate variables and flood event types aligned with well-documented responses to climate change in cold regions (Cockburn & Lamoureux, 2008; Vormoor et al., 2016; Matti et al., 2017; Arp et al., 2020). The significant increase in both mean and maximum spring temperatures matched global climate model predictions for continued warming at high latitudes (Koenigk & Brodeau, 2017; Huo et al., 2022). The increased snow depth also aligned with Pulliainen et al. (2020), who reported rising snow accumulation and snow water equivalent (SWE) in the studied region. Despite this, no significant changes in flood volumes were observed, consistent with previous studies in Fennoscandia (Veijalainen et al., 2010; Korhonen & Kuusisto, 2010; Matti et al., 2017; Lintunen et al., 2024). This lack of change was attributed to longer snowmelt periods, resulting from warming temperatures, which lead to more stable runoff during spring (Fischer & Schumann, 2019; Zhang et al., 2023). Additionally, no significant trends were found in the timing, duration, or interval of flood events, consistent with earlier research in snowmelt-dominated regions (Veijalainen et al., 2010; Vormoor et al., 2016; Matti et al., 2017).

Despite the absence of major trends, low-peak floods (B) increased in both volume and duration, while wavy floods (D) showed a reduction. Both were influenced by rising spring temperatures and deeper snow, conditions expected to intensify across the Northern Hemisphere (Callaghan et al., 2012; Kunkel et al., 2016; Conolly et al., 2019; Pulliainen et al., 2020; Hu et al., 2023). These events also exhibited an increase of occurrence interval indicating that these flood event types are likely to become more common in the future. High one peak floods (A), however, were associated with colder spring temperatures, higher precipitation, and deep snow, consistent with findings that cold springs delay snowmelt and ground thaw, leading to high discharge peaks when the thaw eventually occurrs (Labuhn et al., 2018). Unlike double-peaking floods, single-peak events involved lower temperatures and precipitation during spring, and therefore the rain-on-snow effect could be linked to the wetter conditions seen in double-peaking hydrographs.

Double-peaking floods were connected to warm temperatures and heavy precipitation, both of which are expected to increase at high latitudes due to climate change (Zhang et al., 2023; Blöschl et al., 2017). Rain-on-snow events, which have become more frequent (Fischer & Schumann, 2019), significantly amplify runoff and flood peaks, particularly together with deep snow packs and accelerated melt from warmer spring temperatures. This study found evidence supporting this trend, consistent with previous research (Pulliainen et al., 2020; Zhang et al., 2023) supporting the potential future hydroclimatic regime shift. The findings highlight the complex effects of climate change on flood events and underscore the importance of considering flood event sequencing in assessing the impacts of hydroclimatic shifts. Future research could explore climate teleconnections, such as the North Atlantic Oscillation (NAO) or Arctic Oscillation (AO), to better understand the conditions driving specific flood events (Dahlke et a., 2012; Villarini et al., 2013; Irannezhad et al., 2022).

https://doi.org/10.5194/egusphere-2024-3802
Preprint. Discussion started: 7 January 2025

5.2. Flood event types and morphological response

The study showed that the channel bed's morphological response was strongly influenced by flood event shape and sequences, as well as sediment hysteresis, rather than just flood magnitude. All events exhibited dominant counterclockwise hysteresis, common in sand-bed rivers with upstream sediment supply and bedload-dominated transport (Tananev, 2015; Gunsolus & Binns, 2017). However, the riverbed's morphological response varied with the events hydrograph shape. Single-peak events (A and B) produced distinct erosion and deposition patterns, while double-peaking events (C and D) led to fragmented, small-scale morphological features. Particularly, event B formed classic riffles and pools typical of meandering rivers (Hooke, 2003, Salmela et al., 2022), whereas the reduced sediment transport during second peaks in double-peaking events, also noted in previous flume experiments (Martin & Jerolmack, 2013; Mao, 2018), resulted in complex, small-scale bedforms.

The reduction in sediment transport during the second flood peak has been previously attributed to bed surface reorganization, including coarser sediment exposure (armouring) and infiltration of finer sediments (kinetic sieving), which stabilised the bed, requiring more energy for remobilisation (Curran & Waters, 2014; Dudill et al., 2017; Ferdowsi et al., 2017; Mao, 2018). However, event D displayed clockwise hysteresis during the second peak, suggesting that the riverbed was not able to stabilise between the peaks, enabling faster remobilization of sediments during the second peak and therefore higher TTS compared to other flood events. The fragmented bedforms from double-peaking floods were likely caused by secondary bedforms cannibalizing the larger topography from the first peak, a phenomenon observed in flume studies (Wilbers & Brinke, 2003; Martin et al., 2013). In addition to flood hydrograph shape and hysteresis pattern, sediment particle size played a key role in morphological adjustment. The middle reach with the largest particles (Fig. 5) was eroded only during events A and D, while events B and C caused minimal change in this section of the river. This finding was consistent with earlier research on particle size impact on sediment hysteresis and remobilisation of the sediment particles (Mao, 2012; Malutta et al., 2020).

Despite variations in the modelled runoff volumes, the study identified distinct morphological response patterns for each flood event type. These patterns, shaped by sediment hysteresis, distribution of sediment particle size and flood event sequences, align with findings from previous studies (Martin & Jerolmack, 2013; Gunsolus & Binns, 2017; Mao, 2018). The results highlighted the crucial role of different flood event types in shaping river morphology, revealing that, while event variation likely helps maintain channel equilibrium in long-term, prolonged exposure to certain events—such as high-energy or multi-peaking floods—could disrupt this balance. Such evolution have the potential to destabilise the channel, by altering sediment connectivity, transport processes, and ultimately the morphological structure of the river systems (Bracken et al., 2015; Zhang et al., 2023). Understanding these responses is essential for predicting future river behaviour and managing morphological stability.

5.3. Forecasted hydroclimatic shift and long-term morphological adjustment

This study highlighted the importance of understanding how fluvial sand and gravel-bed systems respond to climatic conditions, particularly by examining the shape and sequencing of flood

https://doi.org/10.5194/egusphere-2024-3802
Preprint. Discussion started: 7 January 2025

hydrographs, which are often overlooked, and more focus is paid on factors like flood volume, timing, or frequency. The results revealed that flood event type and peak sequencing had significant impact on the morphological response of the channel. This together with the observed trends, suggested that even in regions, like the one studied, where hydroclimatic changes are not yet fully visible (Veijalainen et al., 2010; Lintunen et al., 2024), flood event characteristics are evolving with consequences to the river morphology. This and the overserved trends in the hydroclimatic variables underscores that hydroclimatic change is not uniform in space and time across cold regions and rivers should be assessed at the catchment scale to predict future morphological adjustment accurately.

The increase (decrease) of double (single) peaking floods could lead to changes in river system stability, sediment loads, and the spatial distribution of long-term morphological adjustment if certain type of morphological response begin to accumulate (Bracken et al., 2015; Zhang et al., 2023; Blåfield et al., 2024a). Furthermore, previous research findings suggesting that sediment loads in cold regions could rise by 20-30 % for every 1-2 °C increase in temperature (Syvitski et al., 2002; Li et al., 2021) was supported by this study, as the double-peaking floods showed higher geomorphic activity and sediment loads compared to single peaking events of similar volume. This increase together with altered morphological response pattern could eventually lead to sediment transport regime shift. However, the anticipated shift is likely to be a gradual process (Zhang et al., 2023), and the river system may eventually stabilise again. Yet, before stabilizing the shift is likely to challenge the river channel stability, making the long-term morphological adjustment, like meander migration, less predictable (Wohl et al., 2017; Hopwood et al., 2021).

Shifts in the sediment transport regime, along with changes in morphological response and long-term adjustment to evolving flood patterns, are likely to influence the morphological response to summer and autumn precipitation by altering sediment availability and bed form composition. Although these precipitation peaks were not the focus of this study, these seasonal peaks should be considered when predicting and evaluating long-term morphological adjustment of river channels as the distribution of seasonal sediment load is likely shifting towards summer and autumn peaks (Li et al., 2021; Zhang et al., 2023; Blåfield et al., 2024a). This could have significant implications for river ecosystems, flood risk management, and infrastructure planning (Beel., et al., 2021; Gupta et al., 2021; Najafi et al., 2021). Therefore, future research should focus on understanding the combined effects of flood event sequencing, changing precipitation patterns, and sediment transport dynamics under evolving climatic conditions. Long-term monitoring and advanced modelling efforts will be essential to predict the future morphological adjustments of rivers and develop strategies for mitigating these changes' impacts on ecological systems.

6. Conclusions

The findings of this study emphasise the critical role that flood event variability and sequencing play in shaping the morphological response of fluvial sand and gravel-bed systems in cold regions. The results demonstrated that even in areas where hydroclimatic changes are not yet fully visible, flood event characteristics are evolving and remain closely linked to specific climatic conditions. Each

https://doi.org/10.5194/egusphere-2024-3802
Preprint. Discussion started: 7 January 2025

flood event type produced distinct morphological responses, such as the formation of riffles and pools during single-peaking floods, and more fragmented and irregular bed forms in double-peaking floods. Additionally, sediment grain size significantly influenced the spatial distribution of erosion and deposition. The increase of double-peaking flood events, coupled with rising temperatures, could lead to a shift in sediment transport regimes, resulting in heightened geomorphic activity and altered sediment loads. The results underscore the importance of assessing hydroclimatic conditions and flood hydrograph sequences at the catchment scale to accurately predict future morphological adjustment as the impacts of hydroclimatic shift are not uniform across the arctic. Future research should focus on the combined impacts of flood sequences, precipitation patterns, and sediment transport dynamics to develop effective strategies for managing the evolving river systems under climate change. These changes are expected to affect long-term river stability, with significant implications for river ecosystems and flood risk management.

Data availability

The climate data is openly available on Finnish Meteorological Institutes (FMI) data service. The Polmak discharge station data is openly available on Norwegian Water Resources and Energy Directorate (NVE) data service. All the other data is available on request.

Author contribution

Linnea Blåfield – Writing the manuscript, Field work, Methodology, Formal analysis, Visualisation, Funding.

Carlos Gonzales-Inca – Formal analysis, Editing the manuscript

Petteri Alho – Field work, Data curation, Resources, Reviewing the manuscript, Funding, Supervision

Elina Kasvi – Field work, Reviewing the manuscript, Funding, Supervision

Declaration of competing interest

The authors declare that they have no conflict of interest.

Funding

This study was funded by the Kone Foundation (202104246), Digital Waters Flagship – DIWA (359247), HYDRO-RDI-Network (337279), AnthroCliMocs (355018) and the European Union's Next Generation EU recovery instrument (RRF) through the Research Council of Finland projects: Green-Digi-Basin (347701), and HYDRO-RI-platform (346161).

Acknowledgements

The authors would like to thank research assistant Oona Oksanen from the Fluvial and Coastal Research Group (University of Turku) for helping with the data processing, and other group members who have participated in the field work.

References

Arp, C. D., Whitman, M. S., Kemnitz, R., and Stuefer, S. L.: Evidence of hydrological intensification and regime change from northern Alaskan watershed runoff, *Geophysical Research Letters*, 47, e2020GL089186, https://doi.org/10.1029/2020GL089186, 2020.

Beel, C. R., et al.: Emerging dominance of summer rainfall driving High Arctic terrestrial-aquatic connectivity, *Nature Communications*, 12, 1448, https://doi.org/10.1038/s41467-021-21448-7, 2021.

Blåfield, L., Marttila, H., Kasvi, E., and Alho, P.: Temporal shift of hydroclimatic regime and its influence on migration of a high latitude meandering river, *Journal of Hydrology*, 633, 130935, https://doi.org/10.1016/j.jhydrol.2024.130935, 2024a.

Blåfield, L., Calle, M., Kasvi, E., and Alho, P.: Modelling seasonal variation of sediment connectivity and its interplay with river forms, *Geomorphology*, 463, 109346, https://doi.org/10.1016/j.geomorph.2024.109346, 2024b.

Blöschl, G., et al.: Changing climate shifts timing of European floods, *Science*, 357, 588–590, https://doi.org/10.1126/science.aan2506, 2017.

Bracken, L. J., Turnbull, L., Wainwright, J., and Bogaart, P.: Sediment connectivity: a framework for understanding sediment transfer at multiple scales, *Earth Surface Processes and Landforms*, 40, 177–188, https://doi.org/10.1002/esp.3635, 2015.

Callaghan, T. V., Johansson, M., Brown, R. D., et al.: The changing face of Arctic snow cover: A synthesis of observed and projected changes, *AMBIO*, 40, 17–31, https://doi.org/10.1007/s13280-011-0212-y, 2011.

Cockburn, J. M., and Lamoureux, S. F.: Hydroclimate controls over seasonal sediment yield in two adjacent High Arctic watersheds, *Hydrological Processes*, 22, 2013–2027, https://doi.org/10.1002/hyp.6798, 2008.

Connolly, R., Connolly, M., Soon, W., Legates, D. R., Cionco, R. G., and Velasco Herrera, V. M.: Northern Hemisphere snow-cover trends (1967–2018): A comparison between climate models and observations, *Geosciences*, 9, 135, https://doi.org/10.3390/geosciences9030135, 2019.

Curran, J. C., Waters, K. A., and Cannatelli, K. M.: Real-time measurements of sediment transport and bed morphology during channel-altering flow and sediment transport events, *Geomorphology*, 244, 169–179, https://doi.org/10.1016/j.geomorph.2015.06.010, 2015.

Daneshvar Vousoughi, F., Dinpashoh, Y., Aalami, M. T., and Jhajharia, D.: Trend analysis of groundwater using non-parametric methods (case study: Ardabil plain), *Stochastic Environmental Research and Risk Assessment*, 27, 547–559, https://doi.org/10.1007/s00477-012-0599-4, 2013.

https://doi.org/10.5194/egusphere-2024-3802
Preprint. Discussion started: 7 January 2025

Fischer, S., and Schumann, A.: Spatio-temporal consideration of the impact of flood event types on flood statistics, *Stochastic Environmental Research and Risk Assessment*, 34, 1331–1351, https://doi.org/10.1007/s00477-019-01754-8, 2020.

Gaál, L., Szolgay, J., Kohnová, S., et al.: Flood timescales: Understanding the interplay of climate and catchment processes through comparative hydrology, *Water Resources Research*, 48, W04511, https://doi.org/10.1029/2011WR011509, 2012.

Gohari, A., Shahrood, A. J., Ghadimi, S., et al.: A century of variations in extreme flow across Finnish rivers, *Environmental Research Letters*, 17, 124027, https://doi.org/10.1088/1748-9326/aca554, 2022.

Gunsolus, E. H., and Binns, A. D.: Effect of morphologic and hydraulic factors on hysteresis of sediment transport rates in alluvial streams, *River Research and Applications*, 34, 183–192, https://doi.org/10.1002/rra.3240, 2018.

Gupta, H., Reddy, K. K., Gandla, V., et al.: Freshwater discharge from the large and coastal peninsular rivers of India: A reassessment for sustainable water management, *Environmental Science and Pollution Research*, 29, 14400–14417, https://doi.org/10.1007/s11356-021-16811-0, 2022.

Hamed, K. H., and Rao, A. R.: A modified Mann-Kendall trend test for autocorrelated data, *Journal of Hydrology*, 204, 182–196, https://doi.org/10.1016/S0022-1694(97)00125-X, 1998.

Hirvas, H., Lagerbäck, R., Mäkinen, K., et al.: The Nordkalott Project: Studies of Quaternary geology in northern Fennoscandia, *Boreas*, 17, 431–437, https://doi.org/10.1111/j.1502-3885.1988.tb00560.x, 1988.

Hopwood, M. J., Carroll, D., Browning, T. J., et al.: Non-linear response of summertime marine productivity to increased meltwater discharge around Greenland, *Nature Communications*, 9, 3256, https://doi.org/10.1038/s41467-018-05488-8, 2018.

Hooke, J.: River meander behaviour and instability: A framework for analysis, *Transactions of the Institute of British Geographers*, 28, 238–253, https://doi.org/10.1111/1475-5661.00089, 2003.

Huo, R., Li, L., Engeland, K., et al.: Changing flood dynamics in Norway since the last millennium and to the end of the 21st century, *Journal of Hydrology*, 613, 128331, https://doi.org/10.1016/j.jhydrol.2022.128331, 2022.

Hu, Y., Che, T., Dai, L., et al.: A long-term daily gridded snow depth dataset for the Northern Hemisphere from 1980 to 2019 based on machine learning, *Big Earth Data*, 8, 274–301, https://doi.org/10.1080/20964471.2022.2054832, 2023.

Huss, M., Bookhagen, B., Huggel, C., et al.: Toward mountains without permanent snow and ice, *Earth's Future*, 5, 418–435, https://doi.org/10.1002/2017EF000597, 2017.

Irannezhad, M., Ahmadian, S., Sadeqi, A., et al.: Peak spring flood discharge magnitude and timing in natural rivers across northern Finland: Long-term variability, trends, and links to climate teleconnections, *Water*, 14, 1312, https://doi.org/10.3390/w14081312, 2022.

Jhajharia, D., Dinpashoh, Y., Kahya, E., et al.: Trends in temperature over Godavari River basin in Southern Peninsular India, *International Journal of Climatology*, 34, https://doi.org/10.1002/joc.3761, 2014.

Johansson, P.: Late Weichselian deglaciation in Finnish Lapland, *Applied Quaternary Research in the Central Part of Glaciated Terrain*, 47, 2007.

https://doi.org/10.5194/egusphere-2024-3802
Preprint. Discussion started: 7 January 2025

Kasvi, E., Alho, P., Lotsari, E., et al.: Two-dimensional and three-dimensional computational models in hydrodynamic and morphodynamic reconstructions of a river bend: Sensitivity and functionality, *Hydrological Processes*, 29, 1604–1629, https://doi.org/10.1002/hyp.10293, 2015.

Karimaee Tabarestani, M., and Zarrati, A. R.: Sediment transport during flood events: A review, *International Journal of Environmental Science and Technology*, 12, 775–788, https://doi.org/10.1007/s13762-014-0701-x, 2015.

Kociuba, W.: The role of bedload transport in the development of a proglacial river alluvial fan (Case Study: Scott River, Southwest Svalbard), *Hydrology*, 8, 173, https://doi.org/10.3390/hydrology8040173, 2021.

Korhonen, J., and Kuusisto, E.: Long-term changes in the discharge regime in Finland, *Hydrology Research*, 41, 253–268, https://doi.org/10.2166/nh.2010.112, 2010.

Kunkel, K. E., Robinson, D. A., Champion, S., et al.: Trends and extremes in Northern Hemisphere snow characteristics, *Current Climate Change Reports*, 2, 65–73, https://doi.org/10.1007/s40641-016-0036-8, 2016.

Labuhn, I., Hammarlund, D., Chapron, E., et al.: Holocene hydroclimate variability in central Scandinavia inferred from flood layers in contourite drift deposits in Lake Storsjön, *Quaternary*, 1, 2, https://doi.org/10.3390/quat1010002, 2018.

Li, D., Overeem, I., Kettner, A. J., et al.: Air temperature regulates erodible landscape, water, and sediment fluxes in the permafrost-dominated catchment on the Tibetan Plateau, *Water Resources Research*, 57, e2020WR028193, https://doi.org/10.1029/2020WR028193, 2021.

Liébault, F., Laronne, J. B., Klotz, S., and Bel, C.: Seasonal bedload pulses in a small alpine catchment, *Geomorphology*, 398, 108055, https://doi.org/10.1016/j.geomorph.2022.108055, 2022.

Lintunen, K., Kasvi, E., Uvo, C. B., and Alho, P.: Changes in the discharge regime of Finnish rivers, *Journal of Hydrology: Regional Studies*, 53, 101749, https://doi.org/10.1016/j.ejrh.2023.101749, 2024.

Lotsari, E., Dietze, M., Kämäri, M., et al.: Macro-turbulent flow and its impacts on sediment transport potential of a subarctic river during ice-covered and open-channel conditions, *Water*, 12, 1874, https://doi.org/10.3390/w12071874, 2020.

Malutta, S., Kobiyama, M., Borges Chaffe, P.-L., and Bernardi Bonumá, N.: Hysteresis analysis to quantify and qualify sediment dynamics: State of the art, *Water Science and Technology*, 81, 2471–2487, https://doi.org/10.2166/wst.2020.271, 2020.

Mao, L.: The effect of hydrographs on bed load transport and bed sediment spatial arrangement, *Journal of Geophysical Research: Earth Surface*, 117, F03024, https://doi.org/10.1029/2012JF002428, 2012.

Mao, L.: The effects of flood history on sediment transport in gravel-bed rivers, *Geomorphology*, 322, 196–205, https://doi.org/10.1016/j.geomorph.2018.07.017, 2018.

Matti, B., Dahlke, H., Dieppois, B., et al.: Flood seasonality across Scandinavia—Evidence of a shifting hydrograph?, *Hydrological Processes*, 31, 4354–4370, https://doi.org/10.1002/hyp.11365, 2017.

Martin, R. L., and Jerolmack, D. J.: Origin of hysteresis in bed form response to unsteady flows, *Water Resources Research*, 49, 1314–1333, https://doi.org/10.1002/wrcr.20093, 2013.

https://doi.org/10.5194/egusphere-2024-3802
Preprint. Discussion started: 7 January 2025

Meriö, L. J., Ala-aho, P., Linjama, J., et al.: Snow-to-precipitation ratio controls catchment storage and summer flows in boreal headwater catchments, *Water Resources Research*, 55, 4096–4109, https://doi.org/10.1029/2019WR025047, 2019.

Micheletti, N., Chandler, J., and Lane, S.: Near-instantaneous production of digital terrain models in the field using smartphone and structure-from-motion photogrammetry, *EGU General Assembly Conference Abstracts*, EGU2013-10501, 2013.

Mohammadzadeh Khani, H., Kinnard, C., and Lévesque, E.: Historical trends and projections of snow cover over the High Arctic: A review, *Water*, 14, 587, https://doi.org/10.3390/w14040587, 2022.

Najafi, S., Dragovich, D., Heckmann, T., and Sadeghi, S. H.: Sediment connectivity concepts and approaches, *Catena*, 196, 104880, https://doi.org/10.1016/j.catena.2020.104880, 2021.

Tananaev, N. I.: Hysteresis effects of suspended sediment transport in relation to geomorphic conditions and dominant sediment sources in medium and large rivers of the Russian Arctic, *Hydrology Research*, 46, 232–243, https://doi.org/10.2166/nh.2015.202, 2015.

Phillips, C. B., Hill, K. M., Paola, C., et al.: Effect of flood hydrograph duration, magnitude, and shape on bed load transport dynamics, *Geophysical Research Letters*, 45, 8264–8271, https://doi.org/10.1029/2018GL079238, 2018.

Pulliainen, J., Luojus, K., Derksen, C., et al.: Patterns and trends of Northern Hemisphere snow mass from 1980 to 2018, *Nature*, 581, 294–298, https://doi.org/10.1038/s41586-020-2258-0, 2020.

Reesink, A. J., and Bridge, J. S.: Evidence of bedform superimposition and flow unsteadiness in unit-bar deposits, South Saskatchewan River, Canada, *Journal of Sedimentary Research*, 81, 814–840, https://doi.org/10.2110/jsr.2011.69, 2011.

Salmela, J., Kasvi, E., Vaaja, M. T., et al.: Morphological changes and riffle-pool dynamics related to flow in a meandering river channel based on a 5-year monitoring period using close-range remote sensing, *Geomorphology*, 352, 106982, https://doi.org/10.1016/j.geomorph.2019.106982, 2020.

Sen, P. K.: Estimates of the regression coefficient based on Kendall's tau, *Journal of the American Statistical Association*, 63, 1379–1389, https://doi.org/10.1080/01621459.1968.10480934, 1968.

Syvitski, J. P.: Sediment discharge variability in Arctic rivers: Implications for a warmer future, *Polar Research*, 21, 323–330, https://doi.org/10.1111/j.1751-8369.2002.tb00087.x, 2002.

Shrestha, R. R., Bennett, K. E., Peters, D. L., and Yang, D.: Hydrologic extremes in Arctic rivers and regions: Historical variability and future perspectives, in: *Arctic Hydrology, Permafrost and Ecosystems*, edited by: Yang, D., and Kane, D. L., Springer, Cham, 2021.

Vatne, G., Takøy Naas, Ø., Skårholen, T., et al.: Bed load transport in a steep snowmelt-dominated mountain stream as inferred from impact sensors, *Norsk Geografisk Tidsskrift - Norwegian Journal of Geography*, 62, 66–74, https://doi.org/10.1080/00291950802094814, 2008.

Veijalainen, N., Lotsari, E., Alho, P., et al.: National scale assessment of climate change impacts on flooding in Finland, *Journal of Hydrology*, 391, 333–350, https://doi.org/10.1016/j.jhydrol.2010.07.035, 2010.

Viglione, A., Chirico, G. B., Komma, J., et al.: Quantifying space-time dynamics of flood event types, *Journal of Hydrology*, 394, 213–229, https://doi.org/10.1016/j.jhydrol.2010.05.041, 2010.

https://doi.org/10.5194/egusphere-2024-3802
Preprint. Discussion started: 7 January 2025

Vormoor, K., Lawrence, D., Schlichting, L., et al.: Evidence for changes in the magnitude and frequency of observed rainfall vs. snowmelt-driven floods in Norway, *Journal of Hydrology*, 538, 33–48, https://doi.org/10.1016/j.jhydrol.2016.04.061, 2016.

Wenng, H., Barneveld, R., Bechmann, M., et al.: Sediment transport dynamics in small agricultural catchments in a cold climate: A case study from Norway, *Agriculture, Ecosystems & Environment*, 317, 107484, https://doi.org/10.1016/j.agee.2021.107484, 2021.

Williams, G. P.: Sediment concentration versus water discharge during single hydrologic events in rivers, *Journal of Hydrology*, 111, 89–106, https://doi.org/10.1016/0022-1694(89)90254-0, 1989.

Wohl, E.: Connectivity in rivers, *Progress in Physical Geography*, 41, 345–362, https://doi.org/10.1177/0309133317716793, 2017.

Zhang, T., Li, D., Kettner, A. J., et al.: Constraining dynamic sediment-discharge relationships in cold environments: The sediment-availability-transport (SAT) model, *Water Resources Research*, 57, e2021WR030690, https://doi.org/10.1029/2021WR030690, 2021.

Zhang, T., Li, D., East, A. E., et al.: Warming-driven erosion and sediment transport in cold regions, *Nature Reviews Earth & Environment*, 3, 832–851, https://doi.org/10.1038/s43017-022-00362-0, 2022.

Zhang, T., Li, D., East, A. E., et al.: Shifted sediment-transport regimes by climate change and amplified hydrological variability in cryosphere-fed rivers, *Science Advances*, https://doi.org/10.1126/sciadv.adi5019, 2023.